Computers and Chemical Engineering 123 (2019) 184–195

Contents lists available at ScienceDirect

Computers and Chemical Engineering

journal homepage: www.elsevier.com/locate/compchemeng

Demonstration of non-linear model predictive control of post-combustion CO_2 capture processes

S.O. Hauger[a], N. Enaasen Flø[b], H. Kvamsdal[c], F. Gjertsen[a], T. Mejdell[c], M. Hillestad[d,*]

[a] Cybernetica AS, Leirfossv. 27, 7038 Trondheim, Norway
[b] Technology Centre Mongstad (TCM), Mongstad 71, 5954 Mongstad, Norway
[c] Sintef AS, P.O. Box 4760 Torgarden, 7465 Trondheim, Norway
[d] Norwegian University of Science and Technology (NTNU), N-7494 Trondheim, Norway

ARTICLE INFO

Article history:
Received 26 April 2018
Revised 19 September 2018
Accepted 11 December 2018
Available online 27 December 2018

Keywords:
Post-combustion CO_2 capture
Nonlinear model predictive control
Load changes
Pilot plants

ABSTRACT

Nonlinear model predictive control applications have been deployed on two large pilot plants for post combustion CO_2 capture. The control objective is formulated in such a way that the CO_2 capture ratio is controlled at a desired value, while the reboiler duty is formulated as an unreachable maximum constraint. With a correct tuning, it is demonstrated that the controllers automatically compensate for disturbances in flue gas rates and compositions to obtain the desired capture ratio while the reboiler duty is minimized. The applications are able to minimize the transient periods between two different capture rates with the use of minimum reboiler duty.

1. Introduction

One of the main challenges for large scale CO_2 capture deployment, in addition to large capital investment, is the energy cost. For a coal fired power plant it is estimated that carbon capture at the end of the pipe will penalize energy output by approximately 20% (Florin and Fennell, 2010), while House et al. (2009) claim that the penalty cannot be lower than 11%. The energy penalty may even be higher if the operation of the capture plant is not at an optimal operating point. In the present work, optimality refers to minimum specific reboiler duty. For a given capture ratio, there is a lean loading that minimizes the specific reboiler duty. Understripping of the solvent, meaning the lean loading is higher than the optimal, will cost more energy per kg CO_2 captured because more liquid needs to be circulated and thus more cold liquid need to be heated by the reboiler. However, the energy penalty of overstripping, where the lean loading is lower than the optimal, is even more severe. Fig. 12 shows the loss of energy by over- and under-stripping. The optimal point of operation will change with the amount and composition of the flue gas in addition to the capture ratio. As the power plant load is changing, the optimal operating point of the capture plant will change. Manual operation of the capture plant will hardly keep the optimal lean loading at any time, even though an experienced process operator may be able to come close to optimal operation.

For post combustion carbon capture plants, the basic control loops mostly suggested in the literature is one that controls the capture rate by adjusting the solvent fed to the absorber, and another that controls a desorber temperature by adjusting the reboiler duty (Mejdell et al., 2017). There are other basic control loops, such as level controllers of tanks and sumps in addition to pressure and temperature control loops that also need to be present in the plant (Karimi et al., 2012). Tuned properly, these control loops will work well, but after and during load changes or large disturbances, some setpoints need to be adjusted in order to achieve minimum specific reboiler duty (SRD)

There are several studies that have proposed Model Predictive Control (MPC) solutions for post combustion CO_2 capture processes. Luu et al. (2015) propose to use an MPC solution with a linearization of a nonlinear model approximated by a first order dynamics and a dead time. Åkesson et al. (2012) and Prölß et al. (2011) did a simulation study to test nonlinear MPC with one degree and two degree of freedom. He et al. (2017) have implemented both linear and nonlinear MPC, while He et al. (2016) use a linearized model in their MPC solution. Mehleri et al. (2015) designed an advanced MPC scheme to evaluate the controllability of a post-combustion plant in the presence of disturbances associated with the dynamic operation of the power plant.

In the present work an optimal control solution based on nonlinear model predictive control (NMPC) is developed and implemented on two large pilot plants for CO_2 capture. The NMPC

* Corresponding author.
E-mail address: magne.hillestad@ntnu.no (M. Hillestad).

https://doi.org/10.1016/j.compchemeng.2018.12.018
0098-1354/

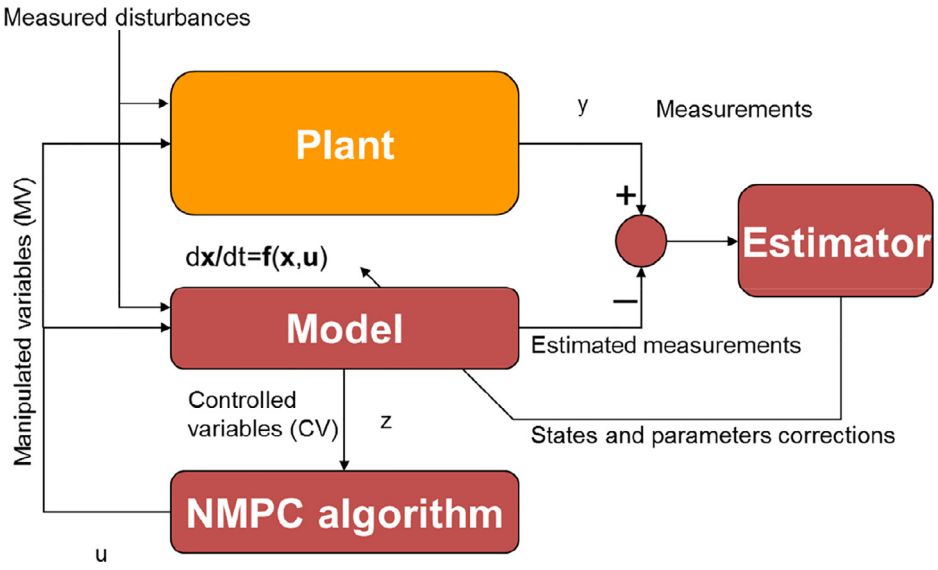

Fig. 1. The NMPC system, consisting of a nonlinear plant model, an online estimator and the NMPC algorithm. (For interpretation of the references to color in this figure, the reader is referred to the web version of this article.)

solution is a 2×2 control scheme, where the objective is to control the reboiler duty to a minimum, while keeping the capture ratio at a given setpoint. The specifications for these two *controlled variables* (CVs) are obtained by manipulating the two manipulated variables (MVs); reboiler duty (or reboiler steam pressure) and solvent flowrate. The solution is implemented on two pilot plants; the Tiller pilot and the Technology Center Mongstad (TCM) test facility. The TCM plant has a capacity of 47,000 Sm^3/h flue gas, while the Sintefs Tiller pilot has a capacity of 250 Sm^3/h. It is demonstrated that the NMPC applications are able to keep the capture ratio at the desired level and at the same time at an optimal lean loading. The main contributions here are (1) formulation and tuning of objective function so that the capture ratio is at the desired value with the use of minimum reboiler duty and (2) the deployment and demonstration of the NMPC solution on two large pilot plants. In addition, the original dynamic model developed by Enaasen Flø (2015) is reduced as described here in Section 2.1.

2. The nonlinear model predictive control application

Model predictive control (MPC) refers to the class of algorithms that compute a sequence of future control inputs in order to optimize the predicted behavior of the process to be controlled. As disturbances enter the process, the optimization is repeated for each sampling time, and therefore only the first part of the input sequence is implemented on the process. Most MPC applications are based on linear step-response models generated by stepping the actual plant. On the other hand, nonlinear model predictive control is based on a nonlinear process model, normally developed from conservation laws and phenomenological relations. These models also need to be validated from plant data, but the plant does not need to be perturbed as much as with linear step-response models. The model, represented by a vector of state variables ($\mathbf{x}$), is expressed as a system of ordinary differential equations.

$$\frac{d\mathbf{x}}{dt} = \mathbf{f}(\mathbf{x}, \mathbf{u}); \quad \mathbf{x}(t_0) = \mathbf{x}_0 \tag{1}$$

The vector $\mathbf{u}$ represents the manipulated variables (MVs) or the handles that we apply to optimize the predicted behavior of the plant. The predicted behavior is represented by the control variables (CVs) that are in general nonlinear functions of the state variables and the MVs; $\mathbf{z} = \mathbf{h}(\mathbf{x}, \mathbf{u})$.

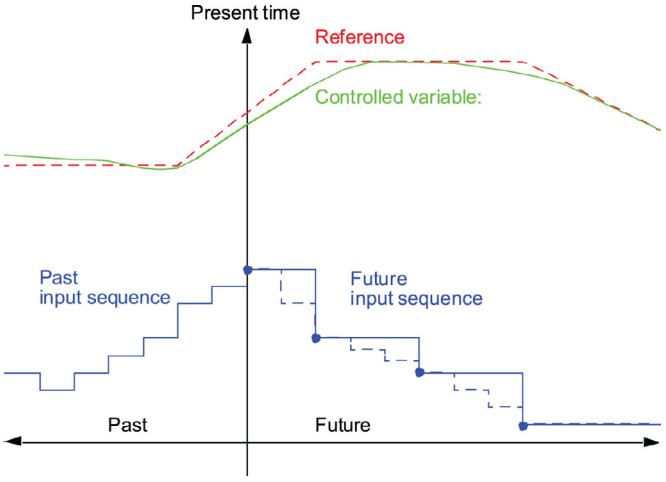

Fig. 2. Illustration of the past (history) and future (prediction horizon) behavior of an NMPC system. The future input (MV) sequence is calculated in order to optimize the behavior of the predicted CVs, which in this illustration is to follow a future reference trajectory. After a complete input (MV) sequence is calculated, only the first value is implemented on the plant. The entire optimization is repeated at every controller sample.

The vector $\mathbf{y} = \mathbf{g}(\mathbf{x}, \mathbf{u})$ is a vector of calculated or estimated measurements that are compared with the actual measurements from the plant. The deviation is applied in an online estimation algorithm to adjust the state variables and model parameters to ensure that the model does not deviate too much from the actual plant. Fig. 1 gives a graphical picture of the functionality of the different blocks.

The objective of the optimization, embedded in the NMPC algorithm, is to calculate the future input sequence that minimizes the future deviations of the controlled variables and their reference trajectory. In addition, the manipulated and control variables may be subject to constraints. This is illustrated in Fig. 2.

The NMPC is implemented in the tool *Cybernetica CENIT*, which includes the properties of the red blocks in Fig. 1. *Cybernetica CENIT* is a widely used tool for NMPC applications, particularly within the polymer, metallurgical industries and batch processing (Singstad, 2017; Kolås and Wasbø, 2010; Elgsæter et al., 2012; Schei, 2007; Foss and Schei, 2005).

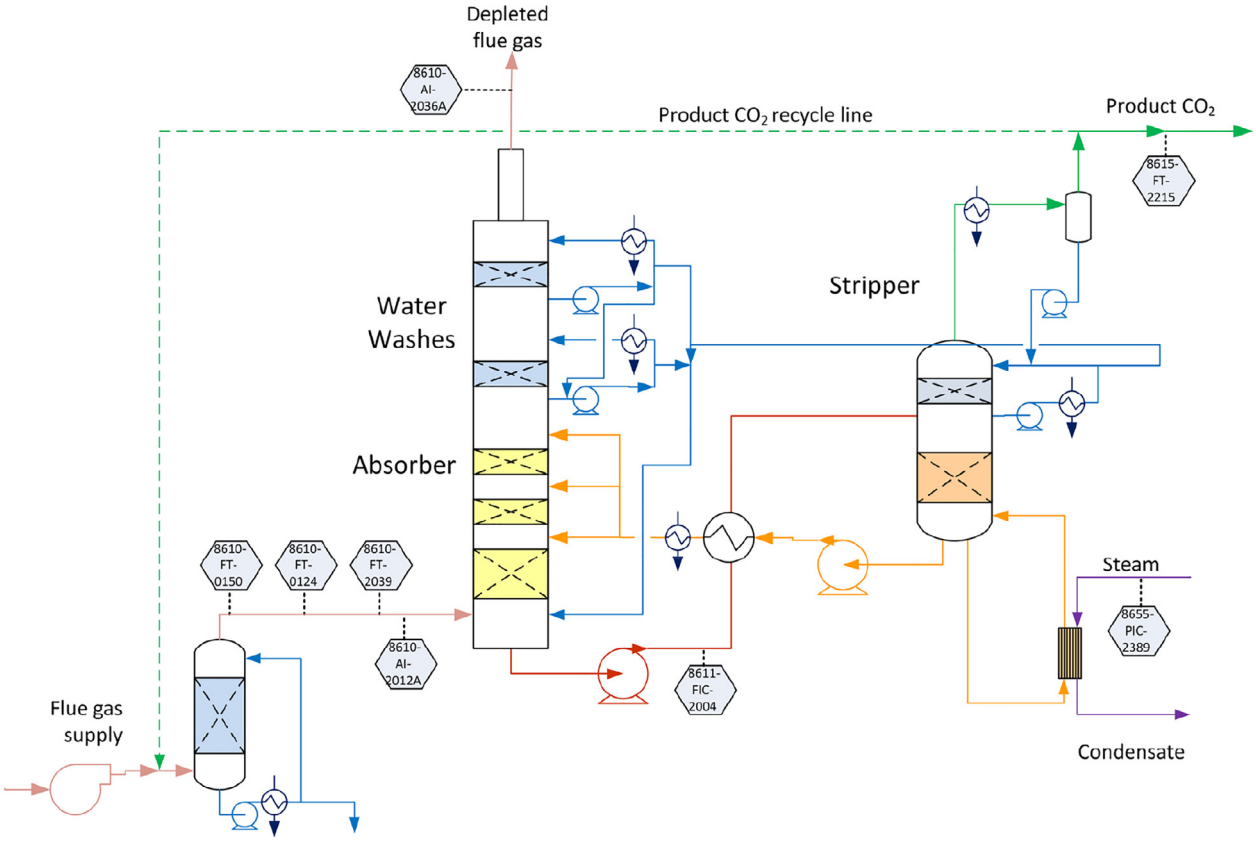

Fig. 3. Simplified process flow diagram of the TCM plant.

2.1. The dynamic process model

The dynamic model of the capture plant is developed by NTNU and SINTEF and a complete description of the model is given by Enaasen Flø (2015). The model is also described in two journal articles (Enaasen Flø et al., 2015, 2016). The model was originally formulated as a system of differential-algebraic equations, containing 1022 dynamic and algebraic states. In order to speed up the computational time, the number of states has been reduced to 448.

All algebraic states are removed by elimination of superfluous boundary conditions of the different process units. The different units are now connected through intermediate input variables instead of algebraic states. In addition, algebraic state variables are eliminated by describing the pressure profiles of the absorber and desorber as an explicit linear interpolation between inlet and outlet pressure. Furthermore, some chemical components are lumped or omitted as they have minor influence on the model predictions; e.g. oxygen and nitrogen are lumped to an inert component in the absorber gas phase, while in the desorber gas phase these components are removed all together. The number of collocation points to describe the axial gradients of the columns and the heat exchanger are reduced. Some detailed thermodynamic relations are substituted by simpler equations, and finally a first order dynamics was introduce in the mass transfer between gas and liquid in order to reduce to stiffness of the ordinary differential equations.

The model reduction has not altered the prediction capacities of the model significantly. The resulting model contains dynamic states only. The model (1) can be integrated as an ordinary differential system, and the code CVODE from Sundials (Hindmarsh et al., 2005) is applied to solve the system. Having a sampling time of 60 s, meaning that the numerical integrator should give a new state vector every 60 s, possibly with new inputs, the model is able to simulate faster than 10,000 times real time. This is fast enough in order to fulfill the NMPC optimization within a sample time of 60 seconds.

A simplified process flow diagram of the TCM plant is shown in Fig. 3. The model of the plant includes the following process units: Absorber, absorber sump, lean/rich cross heat exchanger, desorber, reboiler/desorber sump and overhead condenser. The flue gas fan, direct contact cooler (DCC) system and absorber and desorber water washes are not modeled.

2.2. Model validation against Tiller and TCM data

Both the TCM and Tiller plants are well instrumented. Temperature, pressure, densities and composition measurements are used to validate and fit a few model parameters off-line. A parameter called the wetting factor in the correlation describing the gas liquid contact area is adjusted offline to fit the measurements. An SQP type optimization algorithm is used to estimate some of the most critical model parameters by minimizing the squared sum of deviations between the plant-model and measurements.

Below, two examples of model validation plots are presented. Fig. 4 shows a steady-state temperature profile in the Tiller pilot absorber column. Fig. 5 shows the dynamic responses of the absorber outlet concentration of CO_2 after a step change in the reboiler steam pressure (duty) for the TCM plant.

Similar plots have been constructed for step changes of a number of input variables in order to verify the prediction properties of the dynamic model. The collection of these plots certainly indicates that the model is suitable for use in an NMPC application.

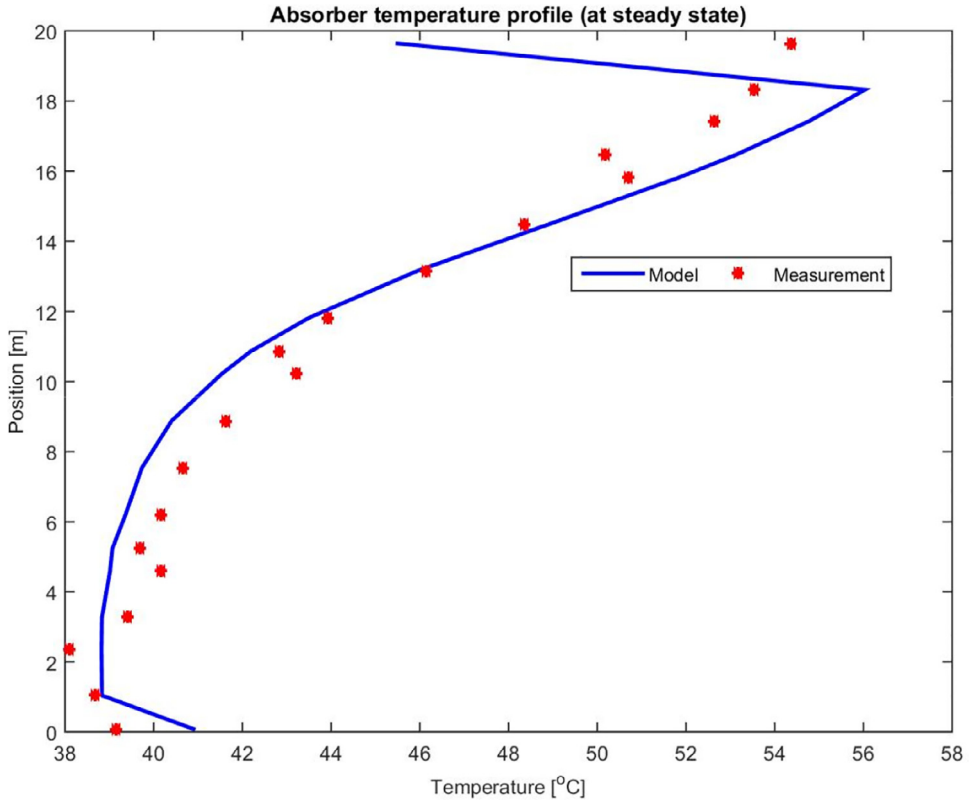

Fig. 4. Example of steady-state temperature profile in the Tiller pilot absorber column.

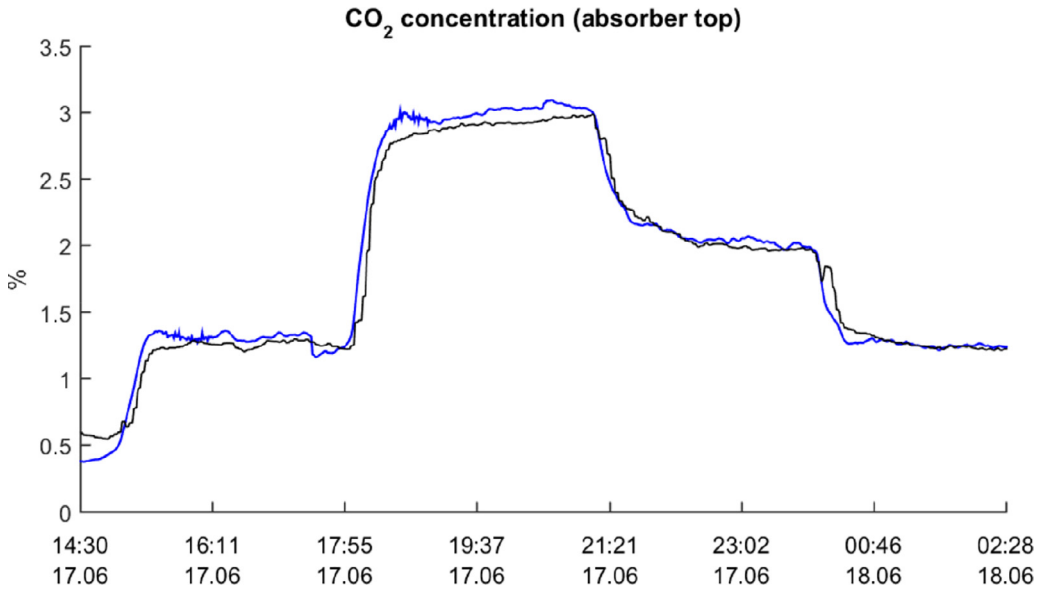

Fig. 5. Example of a dynamic step response from the TCM absorber column, resulting from steps in the reboiler steam pressure. All other inputs are kept constant. The black curve is the measured CO_2 concentration in the depleted flue gas (absorber top), while the blue curve is the ballistic model prediction of the same variable. (For interpretation of the references to color in this figure legend, the reader is referred to the web version of this article.)

2.3. Online model estimation

Based on the off-line fitted model, some critical measurements used for online estimation are selected. That means, which elements of the $\boldsymbol{y}$-vector should be considered in the *Estimator* block in Fig. 1. The most important function of the *Estimator* is to ensure that offset-free control is obtained, which means zero deviation on the average between the selected controlled variables (z) and their corresponding setpoints.

The main controlled variable is the CO_2 capture rate in the absorber, which is closely related to the CO_2 concentration in the absorber top. As can be seen from Fig. 5, the model predictions of this variable seem adequate. However, one should always expect drift between the model and the plant measurement over time, due to un-modeled phenomena, unmeasured disturbances etc.

Different types of online estimators have been investigated, including the Extended Kalman Filter (EKF) for combined state- and

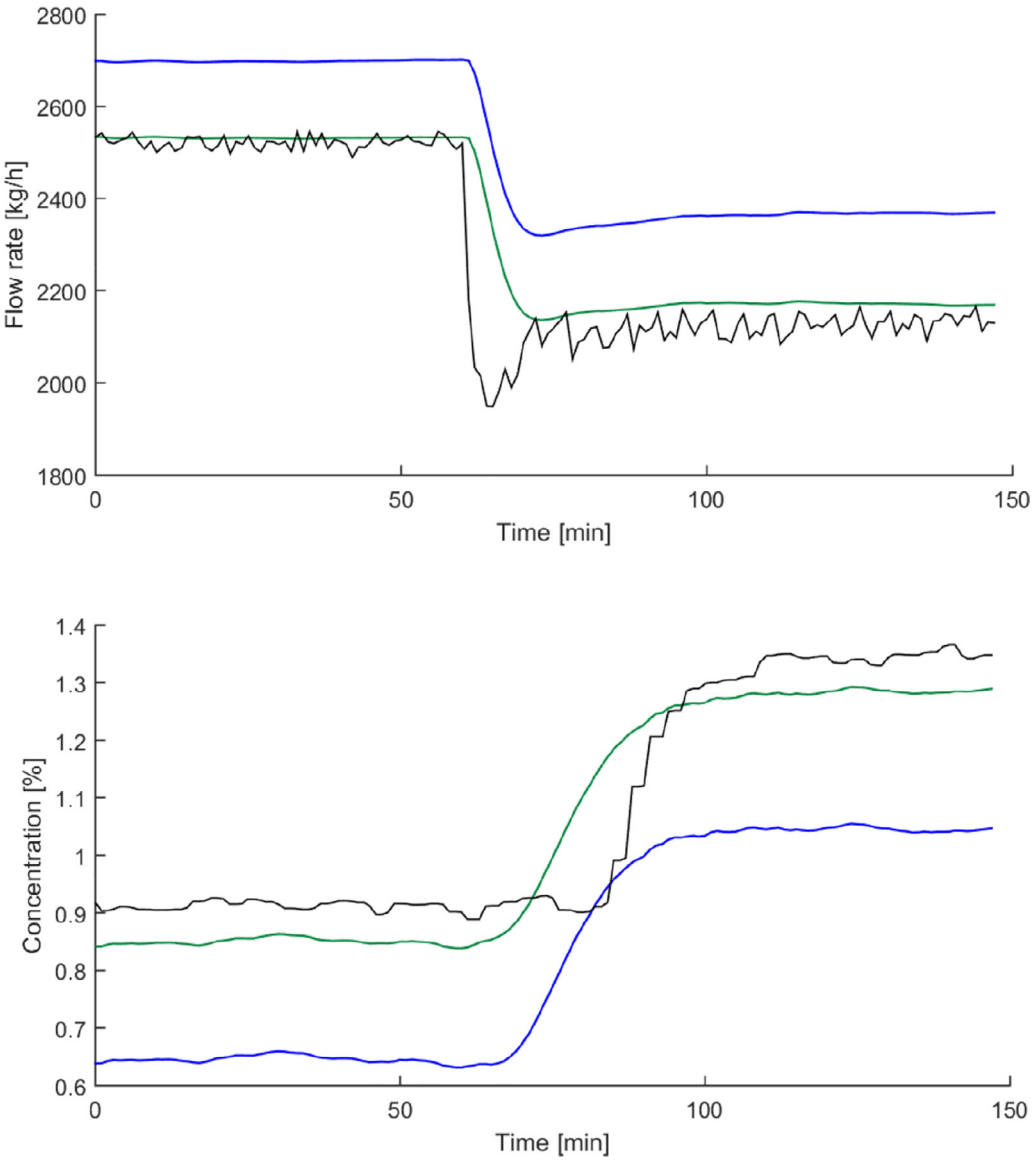

Fig. 6. Online estimation of capture rate at TCM. The model mismatch is almost eliminated for the desorber product flow (upper plot), while minor mismatch may still be seen for the absorber concentrations (lower plot). The black curves represent measured variables, the blue curves represent the non-corrected model values, and the green curves represent the corrected model values. (For interpretation of the references to color in this figure legend, the reader is referred to the web version of this article.)

parameter estimation, which is a built-in component of the Cybernetica CENIT system. Initial tests performed with the EKF algorithm revealed that possible model deviations were not entirely eliminated by updating the physical model parameters. Therefore, a simple updating scheme, based on updating an artificial bias flow of CO_2 in the CO_2 mass balance, was chosen.

It is assumed that the average measurement of CO_2 product flow from the desorber is more reliable than the average GC analysis of CO_2 in the absorber outlet. The measured and estimated CO_2 product flow is therefore compared for close to steady state conditions, and the bias flow is further used to adjust the absorber outlet CO_2 flow. Thus, the absorber CO_2 capture rate is corrected according to the measured desorber CO_2 product flow to get an online updated value of the absorber capture rate. It should be emphasized that the correction from sample to sample is very slow, in order to prevent any dynamic influence on the absorber CO_2 concentration.

The concept is illustrated in Fig. 6 for the TCM plant. The upper plot shows the desorber flow variables. The black curve is the measured product flow of CO_2. The blue curve represents the ballistic (non-updated) calculated product flow from the model, while the green curve shows the online corrected value. Before the change in operating conditions, it is observed that the corrected model value has converged to the measured level. Despite this fact, there is a small deviation between the two corresponding curves representing the absorber top concentrations in the right part of the figure. The reason is that the input- and output measurements for the CO_2 balance are not completely consistent. From the left plot it is also observed that the model bias (average difference between the black and blue curve) is slightly larger after the condition changes, and that the online corrector slowly “pulls” the green estimate towards the black measurement values. Finally, it is observed that the “undershoot” in left side CO_2 flow is not influencing the corrected model value, due to the slow correction.

As the main controlled variable is the CO_2 capture rate in the absorber, CENIT actually controls a capture ratio being equivalent to the CO_2 concentration as indicated by the green curve in the right part of the plot.

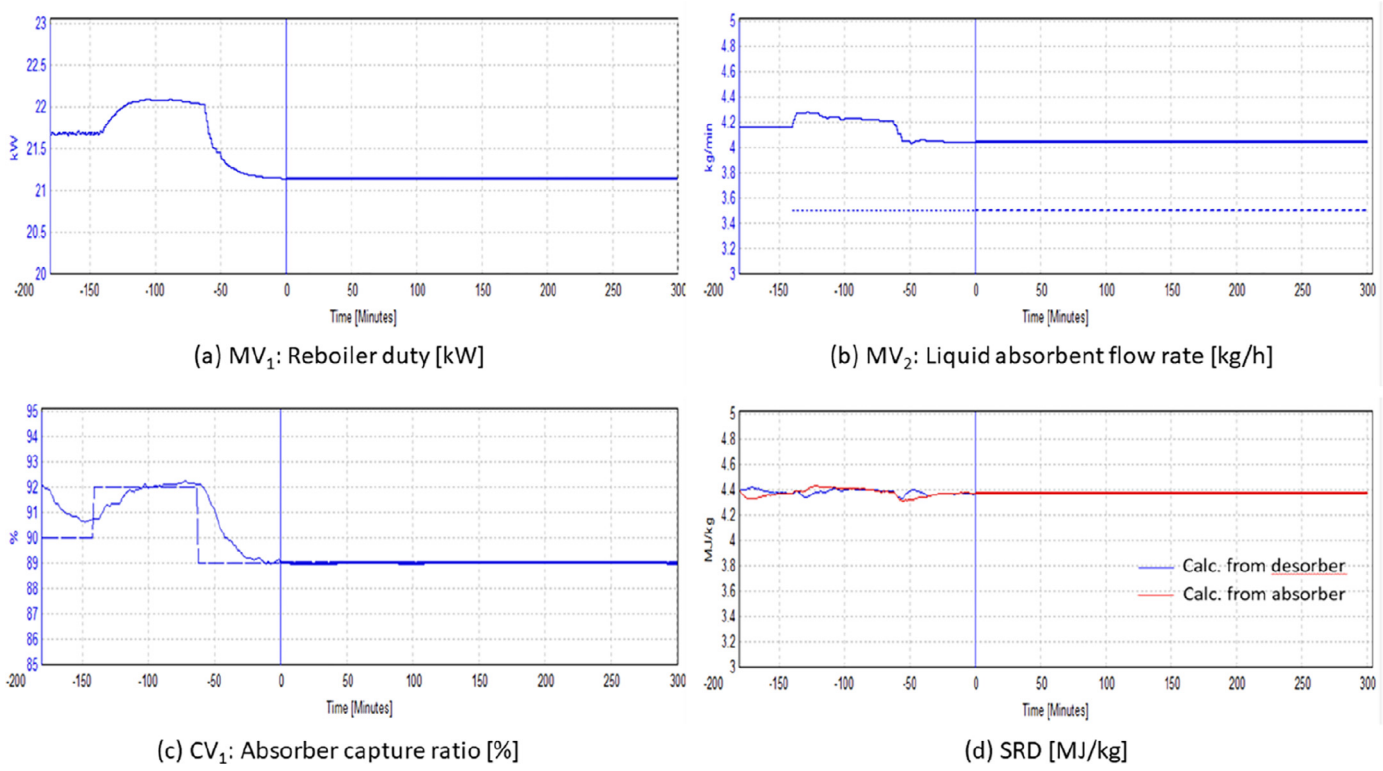

Fig. 7. Controller test 1, Tiller: Changes in capture ratio setpoint. Curves to the left of the vertical line marking time 0 are historical values, while the predictions from CENIT are shown to the right.

2.4. The NMPC control structure

The NMPC objective may be defined by minimizing the quadratic object function (2) below. The first sum represents the penalty of CV setpoint deviations, the second sum is penalty of MV moves and the last sum is soft CV constraints.

$$\min_{\{\Delta\mathbf{u}_{k+j}\},\{\varepsilon_{k+j}\}} J = \sum_{j=1}^{P} \left(\mathbf{z}_{k+j} - \mathbf{z}_{\text{ref},k+j}\right)^T \mathbf{Q}_j \left(\mathbf{z}_{k+j} - \mathbf{z}_{\text{ref},k+j}\right) + \sum_{j=0}^{M-1} \Delta\mathbf{u}_{k+j}^T \mathbf{S}_j \Delta\mathbf{u}_{k+j} + \sum_{j=1}^{P} \mathbf{r}_j^T \varepsilon_{k+j} \tag{2}$$

The objective function is minimized subject to a set of constraints. The model is solved at discrete time steps by the numerical integrator and the control variables are calculated at the same discrete time steps.

$$\mathbf{x_{j+j+1}} = \mathbf{f}(\mathbf{x}_{k+j},\ \mathbf{u}_{k+j},\ \mathbf{v}_k)$$
$$\mathbf{z}_{k+j} = \mathbf{h}\left(\mathbf{x}_{k+j},\ \mathbf{u}\right) \tag{3ab}$$

In addition to the penalty of MV moves, given by $\boldsymbol{S}_j$, there are hard constrains on the manipulated variables both on the actual values and the change from one sample to the next.

$$\mathbf{u}_{\min} \le \mathbf{u}_{k+j} \le \mathbf{u}_{\max}, \quad j = 0, .., M-1$$
$$\Delta\mathbf{u}_{\min} \le \Delta\mathbf{u}_{k+j} \le \Delta\mathbf{u}_{\max}, \quad j = 0, .., M-1 \tag{4ab}$$

Constraints on the controlled variables are implemented as hard constrains with slack variables. The slack variables will prevent the optimization to run into infeasible solutions. With hard constraints both on input and output, it is easy to specify constraints that are infeasible. The control variables may therefore violate their minimum and maximum bounds, but there is a penalty for doing that given by the weights $\boldsymbol{r}_j$.

$$\mathbf{z}_{\min} - \varepsilon_{k+j} \le \mathbf{z}_{k+j} \le \mathbf{z}_{\max} + \varepsilon_{k+j}, \quad j = 1, ..., P$$
$$0 \le \boldsymbol{\varepsilon}_{k+j} \le \boldsymbol{\varepsilon}_{\max}, \quad j = 1, ..., P \tag{5ab}$$

For the applications implemented at the two pilot plants, the elements of the $\boldsymbol{u}$-vector are

1. u_1 or MV_1: The reboiler duty (Tiller application) or the reboiler steam pressure setpoint (TCM application)
2. u_2 or MV_2: The liquid absorbent flow rate. Specified on lean side (Tiller) or rich side (TCM)

The two elements of the z-vector are

1. z_1 or CV_1: The absorber capture rate; calculated by the model and updated online as described in Section 2.3
2. z_2 or CV_2: The reboiler duty

As seen from the MV- and CV lists above, CV_2 is identical to MV_1 (the reboiler duty) in the Tiller case. The mapping function between the MV and the CV (Section 2) is thus trivial;

$$z_2 = h_2(\mathbf{x}, \mathbf{u}) = u_1$$

The operator specifies the setpoint trajectory for CV_1, denoted by $z_{\text{ref},k+j,1}$ for all future samples defined by $j = 1,..,P$, where P is the prediction horizon. Typically, the setpoint is fixed during the entire horizon. Internally in the NMPC, this value is also regarded as a minimum value. At the same time, an artificial, non-obtainable maximum value for CV_2 is specified, which is typically set to zero ($z_{max,2} = 0.0$).

Thus, the controller has apparently been given an unreachable control problem; i.e. to obtain a specific capture rate with "zero" reboiler duty. The NMPC handles this by careful parameterization of the last term in the objective function, where slack variables ε_{k+j} are added to the objective, which allows for $z_{k+j,1} < z_{min,1}$ and $z_{k+j,2} > z_{max,2}$. By assigning linear penalties r_j on the constraint intersections, the optimizer in fact prioritizes between the two constraints: The constraint for CV_1 has sufficiently higher priority than

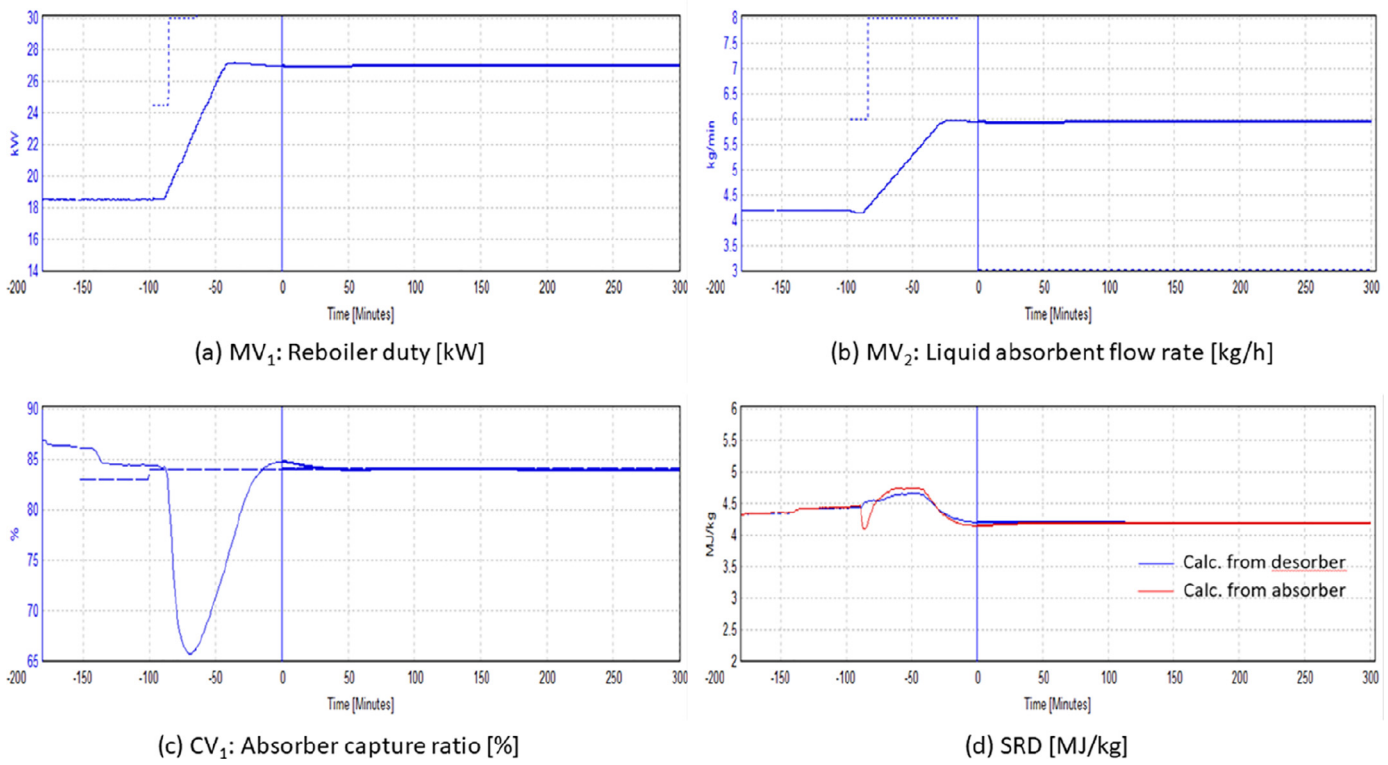

Fig. 8. Controller test 5, Tiller: Changes in flue gas composition from 4.5% to 7.0%. Curves to the left of the vertical line marking time 0 are historical values, while the predictions from CENIT are shown to the right.

the constraint for CV_2, and the optimal solution will fulfill completely the constraint (and setpoint) for the absorber capture rate at steady-state, while at the same time a minimum violation of the duty constraint. In this way, the specified capture rate will always be obtained by the particular combination of MV_1 and MV_2 with the lowest use of energy. This is equivalent to obtaining the specified capture rate with minimum specific reboiler duty (SRD).

Willersrud et al. (2013) discuss solutions for handling unreachable targets in order to obtain production optimization. Their case study deals with maximization of oil flow through an offshore oil and gas production plant, while at the same time respecting targets on critical plant variables like flowline and separator pressures.

The disturbance vector **v** mainly contains the flue gas flow rate and the flue gas composition, in addition to variables like boundary pressures and temperatures.

The controller sampling time is set equal to the model sampling time of 60 s. The objective function has a prediction horizon of 300 min($P = 300$). As indicated in Fig. 2, the future MV moves are not changed every controller sample during optimization, in order to decrease the computational load of the NMPC. In the given configuration, the optimized MVs are fixed (blocked) during four intervals ($M = 4$) through the prediction horizon, starting at future time samples 1, 15, 45 and 90 min ahead. As the optimization is repeated every sample, the simplification introduced by the MV blocking is insignificant as long as the block lengths are selected according to the required closed loop responses.

3. Results

Five different controller tests were planned at both the Tiller and the TCM plant. The tests at the smaller Tiller pilot were scheduled ahead of the tests in the larger test facilities at TCM. Except for some operational differences between the two campaigns, the table below describes the main intentions of the common controller tests.

Controller test 1 is different from tests 2–5 in the sense that reboiler duty or SRD is not minimized in this case. The main intention of this initial test was to verify that the NMPC was able to reach the given setpoints of capture ratio. With reference to the configuration in Section 2, this means that *zero penalty* is put on the constraint intersection for z_2 or CV_2. Thus, there is only one active CV, which is the capture ratio, but still two manipulated variables. Obviously, this configuration does not define a unique steady-state solution for the controller, independent of tuning. In fact, the steady-state combination of the two manipulated variables will be a result of the tuning parameters of the dynamic optimization problem in Eq. (2).

In the below sections, some selected results from both Tiller and TCM pilot plants are presented. All figures are screenshots from the *CENIT* NMPC software, showing the most important variables related to the control objective. The vertical line in each subplot represents present time, with the history trend on the left hand side and the predicted future to the right. See Fig. 2 for comparisons. The screenshots are taken when the plant has settled to nearly steady-state conditions, and this gives rather constant predictions for all variables.

3.1. Closed loop control on the Tiller plant

Fig. 7 shows some set-point changes from controller test 1 at the Tiller plant. As observed from Fig. 7(a) and (b), both reboiler duty (MV_1) and the liquid absorbent flow rate (MV_2) change to obtain new setpoints of the capture ratio (CV_1). The application is able to control the CO_2 capture ratio to set-point as shown in the left figure on second row. Minimum SRD or minimum reboiler duty is not considered in this test.

Fig. 8 shows some results from controller test 5 at Tiller. The flue gas concentration of CO_2 is in this case changed rapidly from

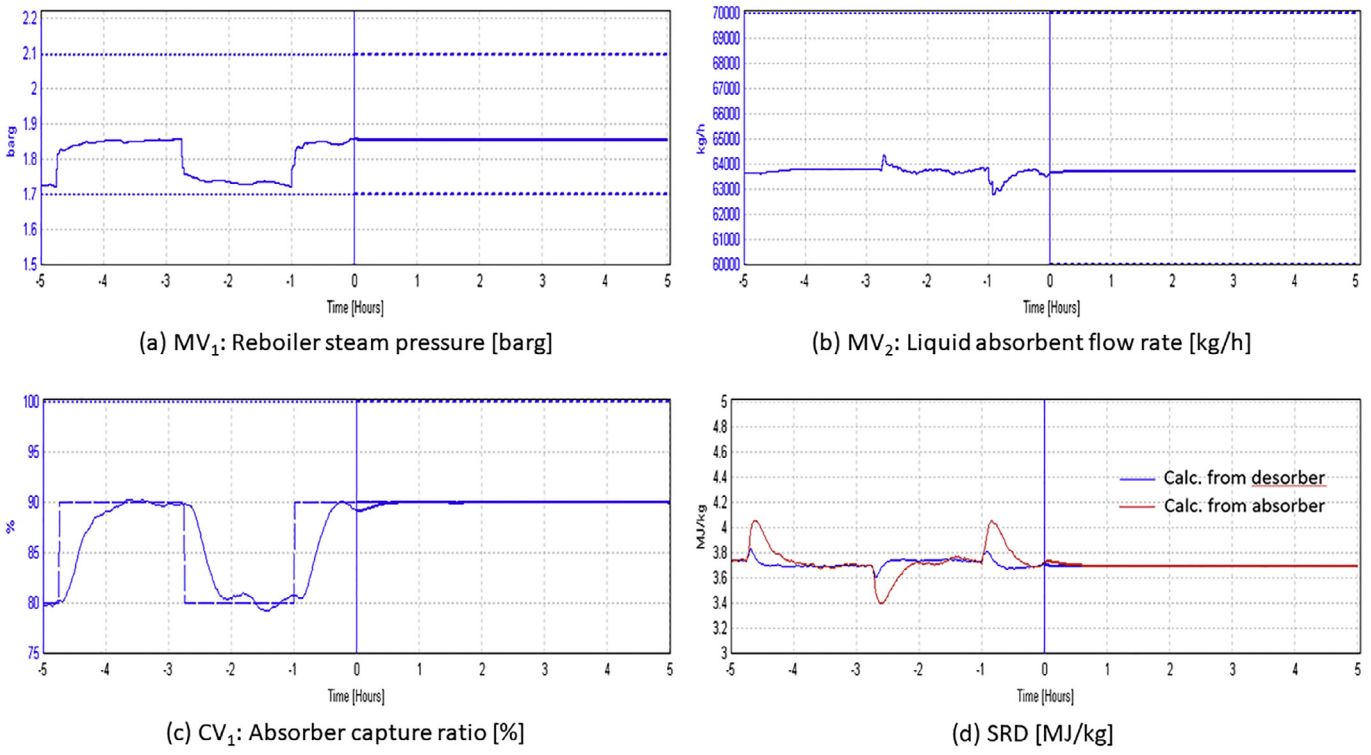

Fig. 9. Controller test 1, TCM – setpoint changes in capture ratio. Curves to the left of the vertical line marking time 0 are historical values, while the predictions from CENIT are shown to the right. The reboiler steam pressure input is given in barg (upper left graph). The mass flow of lean amine is given in kg/hours (upper right graph), the set-point changes (dashed line) and the resulting response (solid line) in capture rate is given in % (lower left graph), and the SRD is given in MJ/kg CO_2 captured (lower right graph).

Table 1
Controller tests at the Tiller and TCM plants.

Controller test #	Activity description	Purpose	Variable to be changed manually	Set-point range	Objective function for NMPC
1	Initial set-point changes of CO_2 capture rate without minimization of reboiler duty	Observe manipulated variables (solvent flow-rate and reboiler duty). Verify changes and response time.	CO_2 capture rate set point	80–90%	Keep CO_2 capture rate at specified set-point.
2	Determination of SRD at base case conditions	Determine minimum SRD for constant base case conditions (gas flow rate and concentration).	None	None	Keep CO_2 capture rate at specific set-point while minimizing reboiler duty
3	Set-point changes in CO_2 capture rate	Check that minimum SRD is achieved for each specific CO_2 capture rate	CO_2 capture rate set point	80–90%	Keep CO_2 capture rate at specific set-point while minimizing reboiler duty
4	Changes in flue gas flow rate	Check that specified CO_2 capture rate and minimum SRD is achieved for each flue gas flow rate	Flue gas flow-rate	60–80% load	Keep CO_2 capture rate at specific set-point while minimizing reboiler duty
5	Changes in flue gas CO_2 concentration	Check that specified CO_2 capture rate and minimum SRD is achieved for each CO_2 gas concentration	Flue gas CO_2 inlet concentration	3.5–13 vol%	Keep CO_2 capture rate at specific set-point while minimizing reboiler duty

4.5% to 7.0%, approximately within two minutes. As observed from Fig. 8(a) and (b), both reboiler duty (MV_1) and the liquid absorbent flow rate (MV_2) changes significantly in order to keep the capture ratio on the desired setpoint, which is set to 84% (left figure on second row). In this case, a more aggressive controller tuning could have led to less transient setpoint deviations for the capture ratio.

Both CV_1 and CV_2 are active in this test (see Table 1), so the final values of MV_1 and MV_2 is meant to be the combination of manipulated variable that gives the lowest value of SRD.

3.2. Closed loop control on the TCM plant

Fig. 9 shows some setpoint changes from controller test 1 at the TCM plant. As explained in Section 2.4, MV_1 is now the setpoint of the reboiler steam pressure, which indirectly controls the reboiler duty. As for the controller test 1 in the Tiller case, only CV_1 is considered in the NMPC criterion.

The operators at TCM were told to make similar changes in capture ratio as the NMPC did. Fig. 10 shows the very first instance of

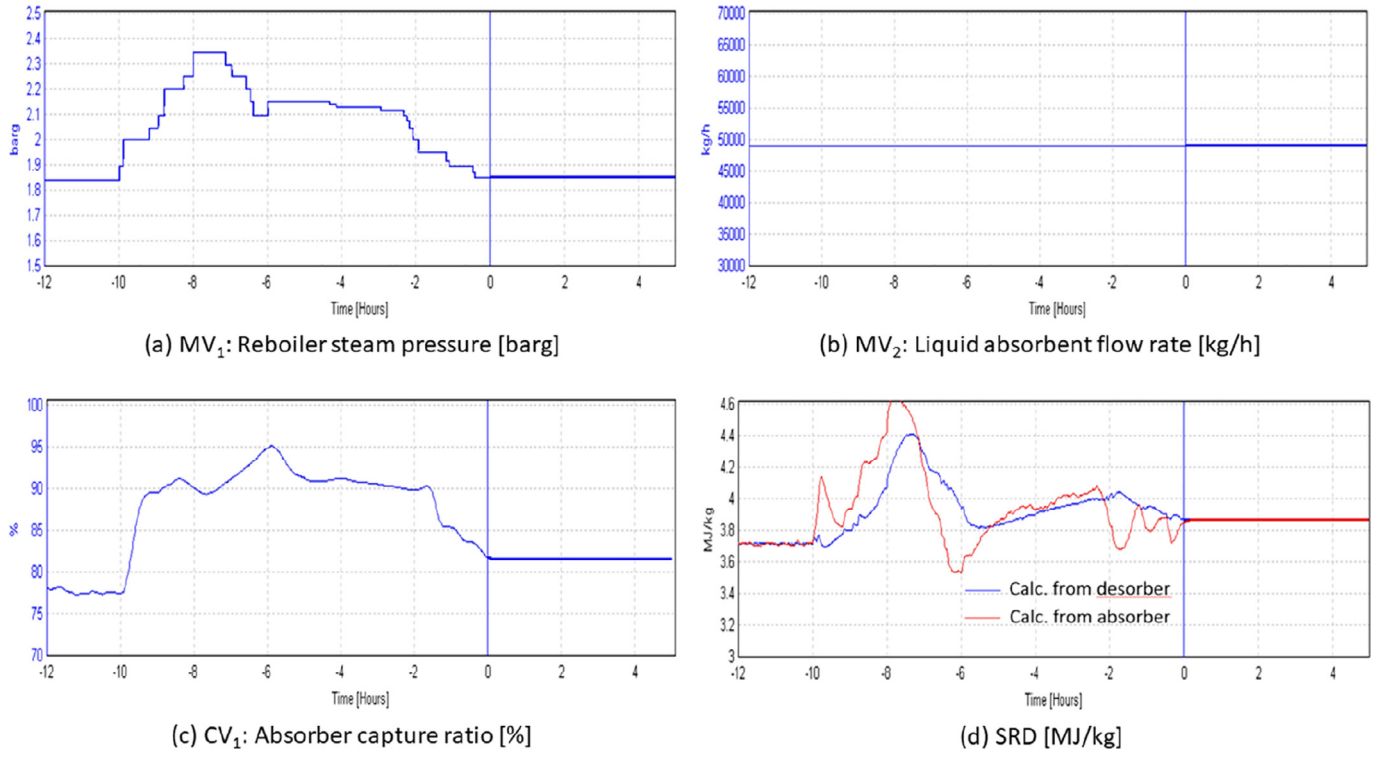

Fig. 10. Example of manual control at TCM to changed capture ratio. Note that only MV_1 was manipulated. Curves to the left of the vertical line marking time 0 are historical values, while the predictions from CENIT are shown to the right.

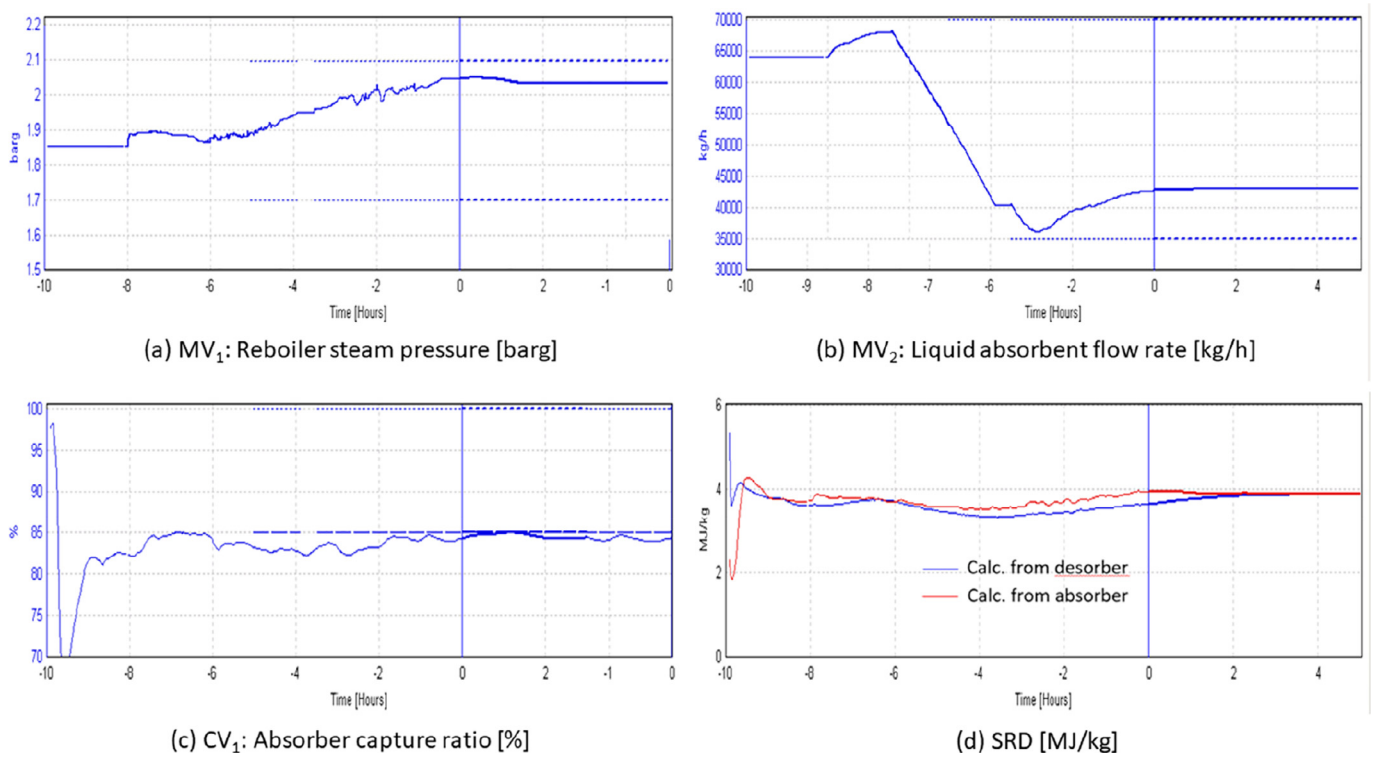

Fig. 11. Controller test 2, TCM – changes in the direction of minimum SRD. Curves to the left of the vertical line marking time 0 are historical values, while the predictions from CENIT are shown to the right.

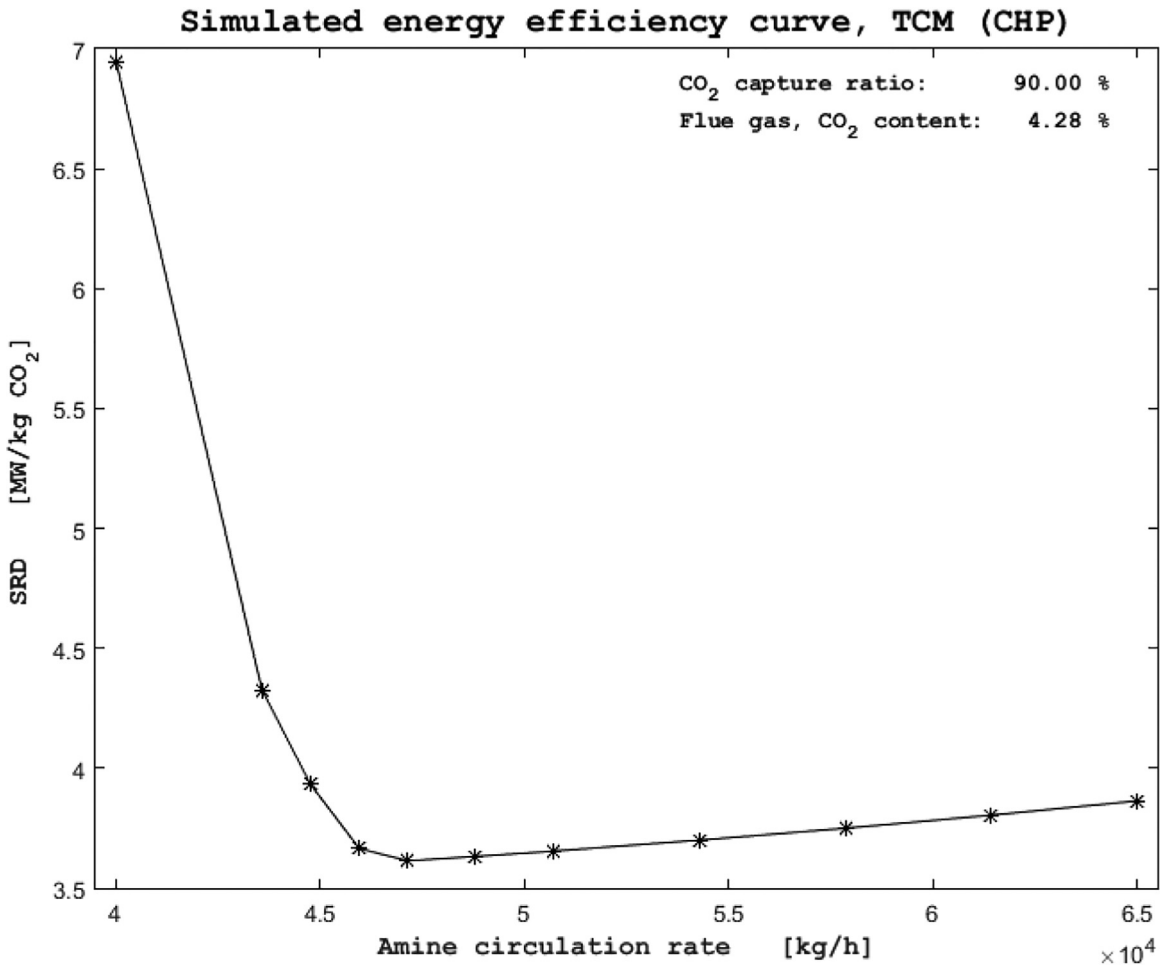

Fig. 12. Typical simulated "U-curve" for the TCM plant. This specific curve is valid for a capture ratio of 90% and a flue gas CO_2 concentration of 4.28%.

manual control, in order to change the capture ratio from about 80–90%. This manual control is less precise than the automatic control shown in Fig. 9. However, it should be emphasized that the operators learnt from test to test, and they were able to improve the manual operation in some of the subsequent tests. Notice also that the second MV (MV_2) was never manipulated, and this was due to the consideration that multivariable manual control was too challenging.

Fig. 11 shows the start of controller test 2. Before the manipulated variables start to change, a base case condition for the TCM plant with capture ratio of 85% was applied. In that particular base case, still a part of controller test 1, only CV_1 is active in the NMPC optimization. The time where CV_2 is activated, approximately at time −7.3 h when MV_2 starts reducing, defines the start of controller test 2. Large reductions in liquid absorbent flow rate are observed when the NMPC searches for minimum SRD.

The exact minimum is not localized, due to some model mismatch which is not completely accounted for through the model updating algorithm described in Section 2.3. Because of the very steep left-hand side of the "U-curve", as shown in Fig. 12, a resulting solvent flow just slightly below the real optimum may increase the SRD significantly. In fact, for this specific TCM test, the optimal decrease in solvent flow should be from the nominal value of approximately 68,000 kg/h to approximately 48,000 kg/h, giving an SRD of about 3.65 MJ/kg CO_2. The controller reduced the flow to approximately 44,000 kg/h, which gave a final SRD close to 4.0 MJ/kg CO_2.

During further plant tests at TCM, an improvement of the minimum SRD control will be tested by using additional measurements in the online estimator algorithm (Fig. 1 and Section 2.3). Utilizing the measured lean and rich CO_2 loading (densities), we can directly adjust the effect of changes in the solvent circulation rate to the CO_2 capture ratio.

Fig. 13 shows results of controller test 4. The flue gas rate is changed in two steps; from 47,000 Sm^3/h to 41,000 Sm^3/h and later from 41,000 Sm^3/h to 35,000 Sm^3/h. Due to operational considerations, a setpoint change in capture ratio, from 85% to 90%, was implemented simultaneously with the second flue gas flow disturbance. As can be seen from Fig. 13(a) and (b), both MVs are reduced, but MV_2 reaches its minimum operator specified value after the second change.

4. Discussion

The NMPC application is in general able to provide a tight control of the CO_2 capture rate at specified set-point both at Tiller and TCM. It is also able to adapt the process to set-point changes in CO_2 capture as was the goal for controller test 3 (see Table 1) in an efficient manner, and the stabilization time is typically less than 1 h at both Tiller and TCM. For controller tests 4 and 5 with changes in flue gas flow input (flow rate and CO_2 concentration, respectively) some deviation in CO_2 capture set-point is typically observed in the transient phase just after the change is implemented, especially for large and/or rapid changes. This is observed in Figs. 8 and 13. However, the specified CO_2 capture rate is always obtained towards the end of the transient period when the process is about to stabilize at new steady state conditions. The stabilization time is in this case up to 1 h. Tuning is possible to

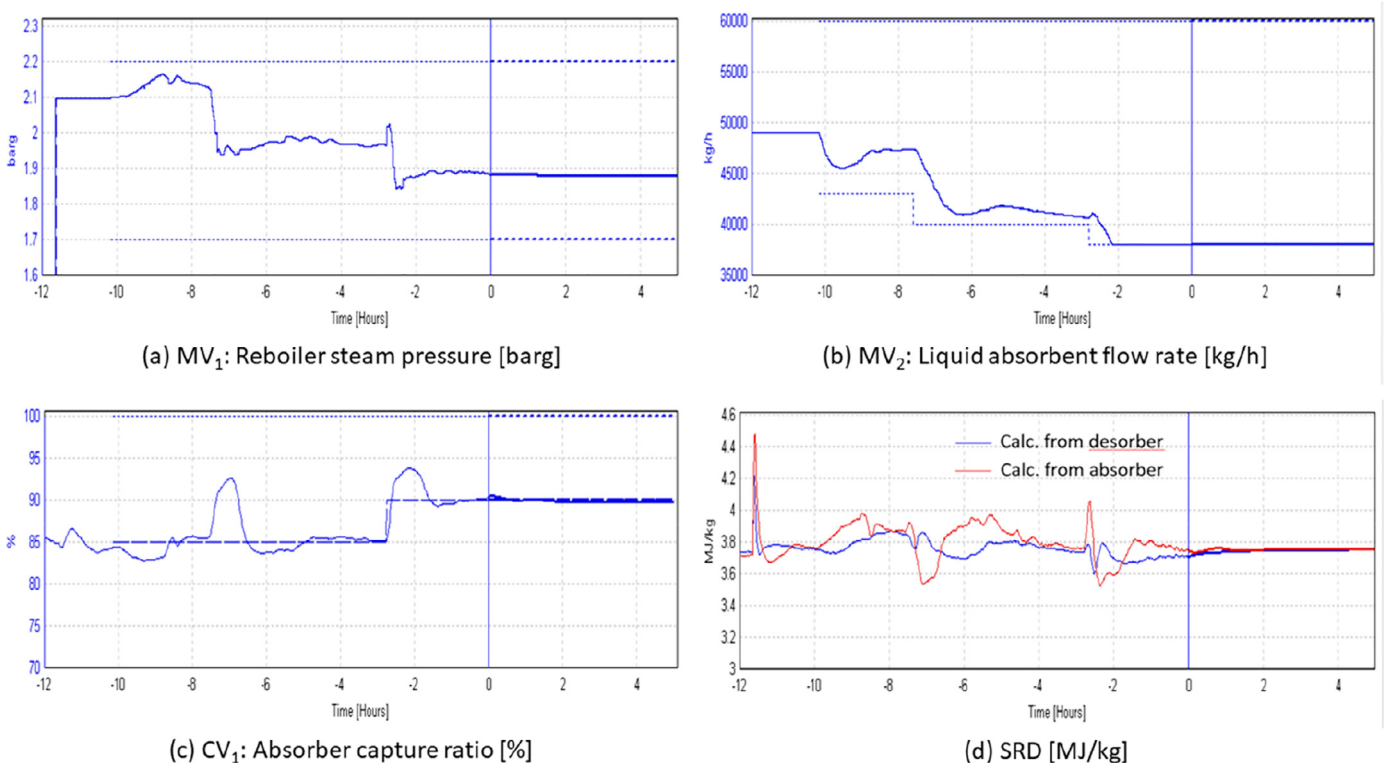

Fig. 13. Controller test 4, TCM – changes in flue gas rate. Curves to the left of the vertical line marking time 0 are historical values, while the predictions from CENIT are shown to the right.

obtain more aggressive controllers, reduce set-point off-set in transient periods and decrease stabilization time, however, a conservative approach was used here in the initial stage. High requirements to closed loop controller response time is highly dependent on the model quality in order to avoid possible overshoots and even controller instability.

The main challenge in the optimization problem is localizing minimum reboiler duty. Hitting the u-curve minimum with optimal solvent flow rate is crucial for localizing minimum SRD. Underestimated solvent flow rate is especially critical with the consequence of over-stripping the solvent. This has a large effect on SRD for even very small off-sets in solvent flow (refer to Fig. 12, left side of SRD minimum). It is evident from the tests conducted at TCM that the application typically resulted in solvent over-stripping which led to suboptimal SRD. Future work will involve software/model improvement to better fit optimal solvent flow rate to experimental results, especially focused on this range of the u-curve. A simple solution where a correction factor to the solvent flow rate was preliminary tested at TCM. The results showed that the SRD could be successfully reduced from about 4 MJ/kg CO_2 to about 3.65 MJ/kg CO_2 which is close to the expected minimum, only by adjusting the solvent flow + 4000 kg/h (9%). An alternative strategy could be to utilize the difference between lean and rich loading for an additional model correction.

In order to evaluate the potential of the NMPC application it should be compared to manual operation. However, making a fair comparison between automatic and manual operation is challenging. The operators at TCM were instructed to make similar changes in CO_2 capture rate as in the tests with NMPC. It was however too challenging to optimize manually two manipulated variables at the time, thus only the steam pressure (reboiler duty) was manipulated manually. This means that the manual tests at TCM were conducted with one degree of freedom only. This fact alone supports use of advanced optimization tools. By comparing the results of manual and automatic control at TCM, it was observed that manual control in general was less precise than the automatic control. Manual control is also largely affected by the strategy of the individual operator on duty, which can lead to large variation in results. However, the operators were able to learn from test to test, and by looking at historic data they were able to improve the manual operation in some of the subsequent tests.

The settling times after setpoint changes of the capture ratio are shown to be faster with the NMPC application compared to manual operation. An indication of this is shown in Figs. 9 and 10. This is an important aspect for pilot plan operation where swift transitions from one operating point to another have large economic benefits. Also when large flue gas flowrate disturbances occurs, the NMPC application is able to compensate the liquid flowrate faster with the use of minimum reboiler duty.

Future work will involve (1) economic optimization in a two level approach (Real Time Optimization) and (2) use of intermediate storage tanks for flexible solvent regeneration.

The two-level optimization routine will minimize energy costs during a 24 h time horizon assuming varying energy prices. The first level will be similar to the approach described in the present work, while the second level will have a much longer prediction horizon and will optimize the average capture rate over the given time horizon under varying energy prices. Utilization of intermediate solvent storage tanks enabling flexible solvent regeneration according to variations in energy process will also be included in the future.

5. Conclusions

In the present work, an optimal control strategy based on nonlinear model predictive control is successfully developed and demonstrated in two different scale CO_2 capture pilot plants. The NMPC application involves 2×2 control where the objective is to minimize reboiler duty while controlling the CO_2 capture rate to specified set-point by manipulating the two controlled variables

reboiler duty and solvent flow rate. The demonstration is fulfilled by completing a rather extensive test program (refer to Table 1) at the Tiller and TCM test facilities in order to validate the NMPC applications ability to control the reboiler duty to minimum while keeping the CO_2 capture rate at specified set-points, but also rejecting disturbances or load changes in flue gas input. It is demonstrated that the NMPC applications are successfully able to keep the CO_2 capture rate at specified set-point, while the minimization of reboiler duty still can be improved.

In large scale facilities, this type of control system may reduce costs with respect to energy consumption and the number of operators. We have seen from the tests that application is able reduce the transient time period from one steady state to another, after changing operating conditions.

Future work will focus on model improvement to better match the experimental u-curve at low lean loadings (low solvent flow rates). Future work will also include extension of the current NMPC application to a two-layer approach in order to enable optimization of energy cost assuming variable energy prices.

References

Åkesson, J., Laird, C.D., Lavedan, G., Prölß, K., Tummescheit, H., Velut, S., Zhu, Y., 2012. Nonlinear model predictive control of a CO_2 post-combustion absorption unit. Chem. Eng. Technol. 35, 445–454. doi:10.1002/ceat.201100480.

Elgsæter, S.M., Kittilsen, P., Hauger, S.O., 2012. Designing large-scale balanced-complexity models for online use. IFAC Proc. 1, 157–162. doi:10.3182/20120531-2-NO-4020.00011.

Enaasen Flø, N., Knuutila, H., Kvamsdal, H.M., Hillestad, M., 2015. Dynamic model validation of the post-combustion CO<inf>2</inf> absorption process. Int. J. Greenh. Gas Control 41. doi:10.1016/j.ijggc.2015.07.003.

Enaasen Flø, N., Kvamsdal, H.M., Hillestad, M., 2016. Dynamic simulation of post-combustion CO_2 capture for flexible operation of the Brindisi pilot plant. Int. J. Greenh. Gas Control 48, 204–215. doi:10.1016/j.ijggc.2015.11.006.

Enaasen Flø, N., 2015. Post-Combustion Absorption-based CO2 Capture: Modeling, Validation and Analysis of Process Dynamics. NTNU, Norway.

Florin, N., Fennell, P., 2010. Carbon Capture Technology: Future Fossil Fuel Use and Mitigating Climate Change. Grantham Institue Climate Change Briefing Paper 3, 20.

Foss, B.A., Schei, T.S., 2005. Putting nonlinear model predictive control into use. In: Proceedings of the Workshop on Nonlinear Model Predictive Control. Freudenstadt, Germany.

He, X., Wang, Y., Bhattacharyya, D., Lima, F.V., Turton, R., 2017. Dynamic modeling and advanced control of post-combustion CO_2 capture plants. Chem. Eng. Res. Des. doi:10.1016/j.cherd.2017.12.020.

He, Z., Sahraei, M.H., Ricardez-Sandoval, L.A., 2016. Flexible operation and simultaneous scheduling and control of a CO_2 capture plant using model predictive control. Int. J. Greenh. Gas Control 48, 300–311. doi:10.1016/j.ijggc.2015.10.025.

Hindmarsh, A.C., Brown, P.N., Grant, K.E., Lee, S.L., Serban, R., Shumaker, D.E., Woodward, C.S., 2005. Sundials: suite of nonlinear and differential/algebraic equation solvers. ACM Trans. Math. Softw. 31, 363–396. doi:10.1145/1089014.1089020.

House, K.Z., Harvey, C.F., Aziz, M.J., Schrag, D.P., 2009. The energy penalty of post-combustion CO_2 capture & storage and its implications for retrofitting the U.S. installed base. Energy Environ. Sci. 2, 193. doi:10.1039/b811608c.

Karimi, M., Hillestad, M., Svendsen, H.F., 2012. Investigation of the dynamic behavior of different stripper configurations for post-combustion CO_2 capture. Int. J. Greenh. Gas Control 7. doi:10.1016/j.ijggc.2011.10.008.

Kolås, S., Wasbø, S.O., 2010. A Nonlinear Model Based Control Strategy for the Aluminium Electrolysis Process, Light Metals. TMS (The Minerals, Metals & Materials Society), Seattle WA February 14-18.

Luu, M.T., Abdul Manaf, N., Abbas, A., 2015. Dynamic modelling and control strategies for flexible operation of amine-based post-combustion CO_2 capture systems. Int. J. Greenh. Gas Control 39, 377–389. doi:10.1016/j.ijggc.2015.05.007.

Mehleri, E.D., Mac Dowell, N., Thornhill, N.F., 2015. Model predictive control of post-combustion CO_2 capture process integrated with a power plant. In: Proceedings of the 12th International Symposium on Process Systems Engineering/25th European Symposium on Computer Aided Process Engineering. Elsevier doi:10.1016/B978-0-444-63578-5.50022-0.

Mejdell, T., Haugen, G., Rieder, A., Kvamsdal, H.M., 2017. Dynamic and control of an absorber - desorber plant at Heilbronn. Energy Procedia 114, 1231–1244. doi:10.1016/j.egypro.2017.03.1378.

Prölß, K., Tummescheit, H., Velut, S., Åkesson, J., 2011. Dynamic model of a post-combustion absorption unit for use in a non-linear model predictive control scheme. Energy Procedia 4, 2620–2627. doi:10.1016/j.egypro.2011.02.161.

Schei, T.S., 2007. Applications of NMPC to industrial batch processes. In: Proceedings of the Keynote Lecture at Workshop on Nonlinear Model Based Control - Software and Applications (NMPC-SOFAP). United Kingdom, Loughborough April 19-20.

Singstad, P., 2017. Industrial batch control applications using nonlinear model predictive control technology based on mechanistic models. In: Proceedings of the Presentation Held at the KoMSO Challenge Workshop – Challenges for Mathematical Modeling, Simulation and Optimization for Advanced Process Control of Batch Processes. Heidelberg *9-10 February*.

Willersrud, A., Imsland, L., Hauger, S.O., Kittilsen, P., 2013. Short-term production optimization of offshore oil and gas production using nonlinear model predictive control. J. Process Control 23, 215–223. doi:10.1016/j.jprocont.2012.08.005.